Modélisation discrète du comportement mécanique de milieux enchevêtrés

Carine Barbier, Rémy Dendievel, David Rodney

Computational approach to the mechanics of entangled materials

Carine Barbier, Rémy Dendievel & David Rodney

SIMAP-GPM2
101, rue de la Physique, Domaine Universitaire, BP 46, 38 402 St-Martin d'Hères Cedex
carine.barbier@gpm2.inpg.fr

Abstract :

We employ a discrete simulation adapted from molecular dynamics techniques in order to study the mechanics of entangled semiflexible fibres. A previous model represent a fibre as a "pearl necklace" [Rodney et al. (2005)]. Successive configurations are obtained by minimizing a potential energy made of linking, bending and interaction terms. This "node" model however imposes limitations both on the computing time (large number of nodes) and on how to model the non-penetrability between fibres. In order to level off these limitations, a new fibre model is developed here, in which the fibres are discretised as a succession of segments. Implementation of friction forces in this "spring" model allows a better understanding of the hysteresis observed experimentally during cyclic compressions of entangled materials.

Résumé :

Nous utilisons une simulation discrète adaptée de techniques de dynamique moléculaire afin d'étudier la mécanique de fibres semiflexibles enchevêtrées. Un précédent modèle représente les fibres à la manière de "colliers de perles" [Rodney et al. (2005)]. Les configurations successives sont obtenues par minimisation d'une énergie potentielle comprenant des termes de liaison, de courbure, et d'interaction entre fibres. Ce modèle « nœuds » nous impose des limitations à la fois sur le temps de calcul (grand nombre de nœuds) et sur la modélisation de la non-pénétrabilité des fibres. Afin de pallier à ces difficultés, un deuxième modèle de fibres est développé ici. Dans celui-ci, les fibres sont discrétisées en "collier de nouilles", par une succession de segments. L'insertion de forces de frottement dans le modèle « segments » permet une étude plus approfondie de l'hystérésis observée expérimentalement lors de compressions cycliques de milieux enchevêtrés.

Key-words :

computational approach; semiflexible fibres; isostatic compression

1 Introduction

Entangled materials are made of fibres arranged together in various manners with no permanent cross-link such as sheep wool, glass wool or steel wool... They exhibit a specific mechanical behavior.

van Wyk (1946) developed a mechanical model for the compression of random fibre networks, based on the statistics of contact formation and fibre bending between contact points. Toll (1998) improved this model by accounting for the fibre orientation. He confirmed the exponent of 3 relating the applied pressure to the volume fraction for 3D random orientations and found an exponent of 5 for 2D networks. Another analytical and statistical approach was developed by Baudequin *et al.* (1999) for large compressions. In this work, in good agreement with experimental results on glass wools, the strain-stress curve follows a power law with an exponent equal to $-3/2$.

Another point of view to probe what happens in fibre assemblies is computer simulations. In the range of large deformations, Durville (2005) used the kinematical beam theory and determined proximity zones between fibres to study the loading curve and the number of contacts

between them during compressions. He obtained results in good agreement with Baudequin model for large deformations and with van Wyk model for small deformations. Fibres can also be modeled by Love-Kirchhoff model, as recently done by Bertails (2006) to perform simulations on realistic hair. This model was also used by Beil *et al*. (2002) to study moderate compressions. Their simulations show a reasonable ability to predict the undetermined constant in van Wyk's equation, although they were limited to a small number of fibres and boundary condition effects were not addressed with precision. In Bertails' and Beil's simulations as in Durville's ones, static and sliding frictions were taken into account. A third manner to model fibres is the one used by Rodney *et al*. (2005) on which our work is based. This "node model" is based on Molecular Dynamics simulations used for polymers. Fibres are discretised by nodes such that the number of nodes per fibre is equal to the fibre aspect ratio (ratio of the length to the diameter of the fibres) and the node diameter is equal to the fibre diameter. The nodal positions are the degrees of freedom of the model. Traction and bending stiffnesses, as well as non-penetrability between fibres are modeled by means of a potential energy. In order to study the entanglement transition, isostatic compressions were performed on initially random fibre configurations. At each compression increment, an energy relaxation is performed to obtain an equilibrium configuration. For all the range of aspect ratios studied (from 10 to 100), three states could be identified. At low density, the fibres do not interact at equilibrium ("free-fiber state"). At higher densities, the fibres strongly interact and lock each other, with a finite number of contacts and an energy that increases rapidly with the density ("entangled state"). Between these two states, there is a "mechanical transition" region where no equilibrium is reached. This method yielded a stress versus relative density in good agreement with van Wyk model for large aspect ratios. But the main restriction of this "node model" is the fact that the computational load increases rapidly with the fibre aspect ratio that was consequently limited to a value of 100, lower than in most real materials, as for example those studied by Poquillon *et al*. (2005).

To reach larger aspect ratios, we develop here a new model in which the fibers are discretised by springs, the number of springs per fibre depending on the accuracy wished for the simulation.

2 Computational model

In this part, we will explain the similarities and the differences between the node model and its evolution: the spring model. In the spring model, the equilibrium distance between two consecutive nodes on a fibre is no longer fixed to the fibre diameter. The dependence between the fibre diameter D and the length ℓ of a spring lies on the bending stiffness of the fibre: since a spring can not bend, not enough springs lead to stiff fibres. This point will be discussed later.

As proposed by Rodney *et al*. (2005), the behavior of the fibre system is modeled using a potential energy. In the case of the present model, even if the forces are still applied to nodes (segment ends), the potential energy is now computed from spring lengths and orientations.

$$E = \sum_{(i,i+1)\, consecutive} \frac{K_S}{2}(1 - \frac{s_{i,i+1}}{\ell})^2 + \sum_{(i-1,i,i+1)\, consecutive} \frac{K_B}{2}(\theta_i - \pi)^2 + \sum_{(i,j) non\, consecutive} \frac{K_I}{2} H(D - r_{i,j})(1 - \frac{r_{i,j}}{D})^{5/2}$$

The above potential energy is composed of three terms. The first one is a linear spring between consecutive nodes that models the resistance either to traction or compression. The second term introduces the bending stiffness by means of angular springs between consecutive segments. The angle of π is the equilibrium angle and forces the fibres to be straight when

no force is applied. The third term models the contacts between fibres and in particular their non-interpenetrability. It is a repulsive potential chosen as Hertz potential, that acts between non-consecutive springs when their distance becomes less than the fibre diameter D, which is implied by the Heaviside step function $H(x)$. The distance between springs $r_{i,j}$ is that of closest approach, computed according to the method of Kumar *et al.* (2001). Depending on the configuration, the vector of closest approach is either perpendicular to the two springs or links one spring to one end of the other spring (see fig 1), or it may link one end of a spring to an end of the other spring.

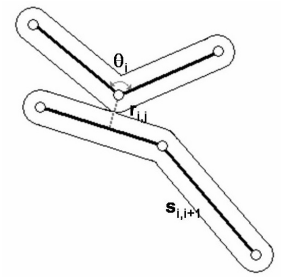

Figure 1: Schematic representation of spring-spring interaction.

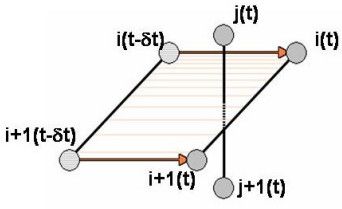

Figure 2: Test on spring displacement: does a spring cross the surface created by the motion of any other spring?

The main advantage of discretising the fibres by springs is to decrease the number of degrees of freedom per fibre. As mentioned in the literature (see Kumar *et al.* (2001); Bertails (2006)), the drawback of this method is to lead to spring crossings between two simulation steps. Determining whether the motion of a given spring intersects any other spring is therefore of crucial importance for the integrity of the simulation. For this reason, we test during the first 200 relaxation steps of each compression increment whether a spring crosses the surface created by the motion of any other spring, as illustrated in fig 2. In such a case, the time step is decreased and all spring displacements are recomputed. This test is not performed for all simulation steps because it strongly increases the computational load and it is of importance only during the first simulation steps of each increment.

We also implemented a Coulomb-like friction at contacts points, in order to study the influence of sliding between fibres. We apply a friction force with a norm equal to the repulsive normal force between springs multiplied by a friction coefficient. It is applied in the plane perpendicular to the repulsive normal force with a direction opposite to the relative velocity of the considered spring with respect to the other contact spring.

In order to validate this model, we compared its predictions with that of the node model. As shown in fig 3, we first studied the bending behavior of a single fibre clamped at one end and subjected to a vertical force F applied to its other end. We performed simulations for a fibre with an aspect ratio of 20 and compared these results with Finite Element simulations. The most important result is the good agreement all methods all over the applied force range. This shows that the fibre follows a power law well-known in beam theory, $\frac{\delta}{D} = \frac{F}{3}(\frac{L}{D})^3\kappa$. Moreover, in both spring and node models, the bending stiffness can be computed analytically: $\kappa = \frac{D^2}{K_B\ell}(1-\frac{\ell}{L})(1-\frac{\ell}{2L})$ where ℓ is spring length and L is the fibre length between its two extremities. Since the stiffness depends on the spring length, equal to D in the case of the node model, the bending coefficient K_B in the spring model was made dependent on the number of springs per fibre in order to keep the same κ. An observation is that a fibre described by only 4 springs is slightly stiffer for deflection larger than six times the fibre diameter. But we have

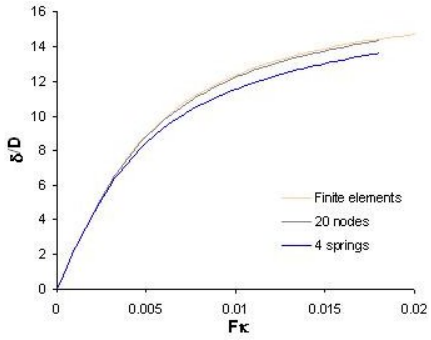

Figure 3: Dimensionless deflection as a function of dimensionless applied force for a fibre of aspect ratio 20, clamped at one end and subjected to a vertical force F applied to its other end.

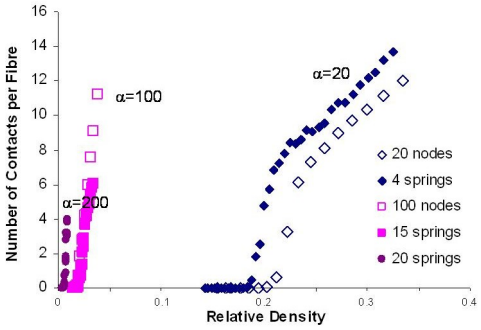

Figure 4: Number of contacts per fibre as a function of relative density for various aspect ratios α; diamond: $\alpha = 20$, square: $\alpha = 100$, circle: $\alpha = 200$. Open symbols correspond to the node model, filled symbols to the springs model.

only performed simulations in the small deformations range, i.e. in the range of deformations where the spring model and the Finite Elements are in good agreement.

We also simulated incremental isostatic compressions of fiber systems. Different assemblies of homogeneous aspect ratio fibres are initially placed in the cell and oriented at random. We studied fibre arrangements by following the number of contacts per fibre during the compressions with respect to the relative system density, as shown in Fig. 4. The shape of the curves obtained with the both models are nearly identical. We can conclude that for fibres of aspect ratio equal to 20, only 4 springs can be used to model a fibre, instead of 20 nodes. In the same manner, fibres with a aspect ratio of 100 can be modeled by only 15 springs, leading to a large decrease in the number of degrees of freedom in the simulation. We can also see that it is possible with the spring model, to perform simulations of fibres of aspect ratio up to 200, which is close to the aspect ratio of 250 measured by Masse *et al*. (2006) for steel wools.

3 Results and discussion

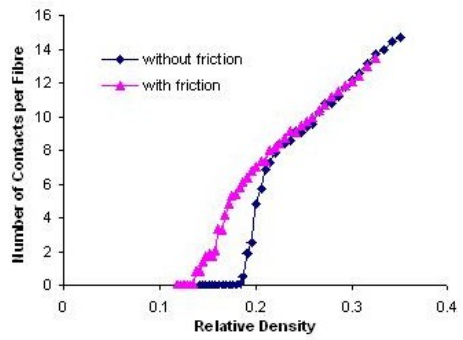

Figure 5: Contacts per fibre as a function of the relative density during isostatic compressions of 4-spring fibres of aspect ratio 20 with and without friction.

In this part, we discuss the first results obtained with the spring model concerning the influence of sliding friction and hysteresis between successive compressions and relaxations. We studied the influence of sliding friction during isostatic compressions of an entangled assembly

of fibres of aspect ratio equal to 20, modeled with 4 springs. As shown in fig 5, the simulations were performed with friction (friction coefficient of 0.5) and without friction. A first result is that applying friction forces shifts the transition (i.e. the region of rapid increase of contact number) to lower densities and lower contact numbers. Another result is that after the transition, there is superposition of the curves. This is due to the fact that beyond the transition the fibres lock each other and cannot move, and therefore cannot slide on each other. Thus, the influence of sliding friction on the number of contacts is significant only during the mechanical transition. Nevertheless, sliding friction leads to an increase of stress from about 100% after the transition to about 10% for the highest simulated relative density.

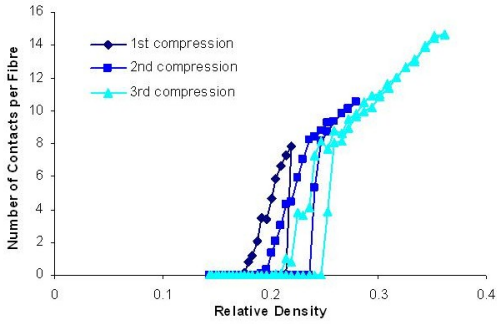

Figure 6: Contacts per fibre as a function of relative density for 4-spring fibres of aspect ratio 20.

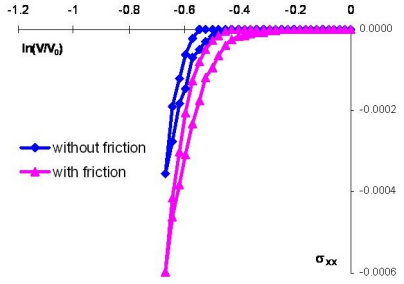

Figure 7: Stress-strain curve of the second compression/relaxation cycle either with friction or without friction (friction coefficient of 0.5).

We are also interested in the hysteresis that is observed experimentally during compression/relaxation cycles (see Ref. Poquillon *et al*. (2005)). This phenomenon may be attributed either to the friction between fibres and/or irreversible fibre rearrangements. We performed cycles of compressions followed by relaxations, going to larger compression rates at each cycle. Relaxations were performed by incrementally increasing the cell volume until it was back to its initial value. The resulting number of contacts per fibre as a function of the relative density is presented in fig 6 for fibres made of 4 springs with an aspect ratio of 20. The curves are shown for the first three cycles. They follow a master curve that corresponds to a one-way compression, as mentioned by Masse *et al*. (2006) in experimental compressions of steel wools. In fig 7, we plotted the stress-strain curve of the second compression/relaxation cycle either with or without friction. In both cases, an hysteresis is visible. As already mentioned above, the compression with friction is shifted to lower deformations. But most importantly, there is hysteresis even without friction. We can therefore conclude that hysteresis is at least partly due to irreversible rearrangements of the fibres. It is also worth noting that, even if the curves obtained for single compressions are superposed beyond the transition (fig 5), sliding friction has an effect on the fibres arrangement which explains the difference in the stress between the two curves in fig 7 even after the transition.

4 Conclusion

This work shows that the number of degrees of freedom of a fibre assembly can be reduced by discretising the fibres by springs without any loss of reliability. Indeed for isostatic compressions, results obtained with the spring model are in good agreement with those obtained with the node model in the range of small deformations for fibres of various aspect ratios. Moreover, the study of sliding friction shows that sliding influences the system mainly during the mechanical

transition, i.e. when the fibres start to be in contact and the network is not already locked. It would be interesting to implement in our model static friction forces. Finally the simulations of compresion/relaxation cycles show that hysteresis is partly due to irreversible rearrangements of the fibres. Sliding friction has not a strong influence on this phenomenon. One perspective of this work is to perform simulations based on realistic initial configurations. To do this, images of steel wools have been obtained, in collaboration with J.P. Masse and L. Salvo, by using 3D X-ray tomography. Our aim is to skeletonise and discretise in springs the X-ray tomography images. We would then be able to perform simulations based on realistic initial configurations extracted from real samples.

References

Baudequin, M., Ryschenkow, G., Roux, S. 1999 Non-linear elastic behavior of light fibrous materials *Eur. Phys. J. B* **12** 157-162

Beil, N.B., Roberts, W.W. 2002 Modeling and Computer Simulation of the Compressional Behavior of Fiber Assemblies, Part I: Comparison to van Wyk's Theory *Textile Res. J.* **72** 341-351

Beil, N.B., Roberts, W.W. 2002 Modeling and Computer Simulation of the Compressional Behavior of Fiber Assemblies, Part II: Hysteresis, Crimp, and Orientation Effects *Textile Res. J.* **72** 375-382

Bertails, F. 2006 Simulation de chevelures virtuelles *Thèse,INP GRENOBLE*

Durville, D. 2005 Numerical simulation of entangled materials mechanical properties *J. Mat. Sc.* **40** 5941-5948

Kumar, S., Larson, R.G. 2001 Brownian dynamics simulations of flexible polymers with spring-spring repulsions *J. Chem. Phys.* **114** 6937-6941

Masse, J.P., Salvo, L., Rodney, D., Bréchet, Y., Bouaziz, O. 2006 Influence of relative density on architecture and mechanical behaviour of steel metallic wool. *Scripta Materialia* **54** 1379-1383

Poquillon, D., Viguier, B., Andrieu, E. 2005 Experimental data about mechanical behaviour during compression test for various matted fibres. *J. Mat. Sc.* **40** 5963-5970

Rodney, D., Fivel, M., Dendievel, R. 2005 Discrete Modeling of the Mechanics of Entangled Materials. *Phys. Rev. Lett.* **95** 108004

Toll, S. 1998 Packing Mechanics of Fiber Reinforcements. *Polymer Engineering and Science* **38** 1337-1350

van Wyk, C.M. 1946 Note on the compressibility of wool. *J. Textile Inst.* **37** T285-T292